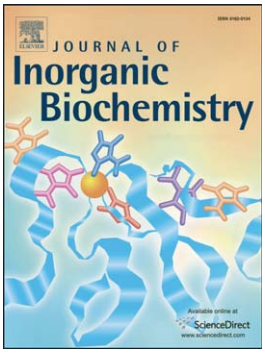

Nanosized mesoporous metal–organic framework MIL-101 as a nanocarrier for photoactive hexamolybdenum cluster compounds

Anastasia M. Cheplakova, Anastasiya O. Solovieva, Tatiana N. Pozmogova, Yuri A. Vorotnikov, Konstantin A. Brylev, Natalya A. Vorotnikova, Elena V. Vorontsova, Yuri V. Mironov, Alexander F. Poveshchenko, Konstantin A. Kovalenko, Michael A. Shestopalov

PII: S0162-0134(16)30395-6
DOI: doi:10.1016/j.jinorgbio.2016.11.014
Reference: JIB 10114

To appear in: *Journal of Inorganic Biochemistry*

Received date: 2 August 2016
Revised date: 3 November 2016
Accepted date: 8 November 2016

Please cite this article as: Anastasia M. Cheplakova, Anastasiya O. Solovieva, Tatiana N. Pozmogova, Yuri A. Vorotnikov, Konstantin A. Brylev, Natalya A. Vorotnikova, Elena V. Vorontsova, Yuri V. Mironov, Alexander F. Poveshchenko, Konstantin A. Kovalenko, Michael A. Shestopalov, Nanosized mesoporous metal–organic framework MIL-101 as a nanocarrier for photoactive hexamolybdenum cluster compounds, *Journal of Inorganic Biochemistry* (2016), doi:10.1016/j.jinorgbio.2016.11.014

Nanosized mesoporous metal–organic framework MIL-101 as a nanocarrier for photoactive hexamolybdenum cluster compounds

Anastasia M. Cheplakova[a,bc], Anastasiya O. Solovieva[c†], Tatiana N. Pozmogova[b,c], Yuri A. Vorotnikov[a], Konstantin A. Brylev[a,b,c], Natalya A. Vorotnikova[a], Elena V. Vorontsova[d], Yuri V. Mironov[a,b], Alexander F. Poveshchenko[c], Konstantin A. Kovalenko[*a,b], Michael A. Shestopalov[*a,b,c]

[a] *Nikolaev Institute of Inorganic Chemistry SB RAS, 3 Acad. Lavrentiev ave., 630090 Novosibirsk, Russian Federation, E-mail: k.a.kovalenko@niic.nsc.ru, shtopy@niic.nsc.ru*

[b] *Novosibirsk State University, 2 Pirogova st., 630090 Novosibirsk, Russian Federation*

[c] *Scientific Institute of Clinical and Experimental Lymphology, 2 Timakova st., 630060 Novosibirsk, Russian Federation*

[d] *The Institute of Molecular Biology and Biophysics, 2/12 Timakova st., 630117 Novosibirsk, Russian Federation*

Keywords: Molybdenum clusters / MIL-101 / Luminescence / Singlet oxygen / Hep-2 cells / Phototoxicity

ABSTRACT

Inclusion compounds of photoluminescent hexamolybdenum cluster complexes in the chromium terephthalate metal-organic framework, MIL-101 (MIL, Matérial Institut Lavoisier) were successfully synthesized in two different ways and characterized by means of powder X-Ray diffraction, chemical analysis and nitrogen sorption. Some important functional properties of hexamolybdenum cluster complexes for biological and medical applications, in particular singlet oxygen generation ability, luminescence properties, cellular uptake behavior and cytotoxicity were studied. It was revealed that the inclusion compounds possessed significant singlet oxygen generation activity. The materials obtained showed a low cytotoxicity, thus allowing them to be used in living cells. Confocal microscopy of human larynx carcinoma (Hep-2) cells incubated with the inclusion compounds showed that MIL-101 performed as a nanocarrier adhering to the external cell membrane surface and releasing the cluster complexes which that penetrated into the cells. Moreover, photoinduced generation of reactive oxygen species (ROS) in Hep-2 cells incubated with inclusion compounds was demonstrated. The cluster supported on MIL-101 was shown to possess *in vivo* phototoxicity.

1 Introduction

Octahedral molybdenum cluster complexes with the general formula $[\{Mo_6X_8\}L_6]^{2-}$ (X – Cl, Br or I; L – an organic or inorganic ligand) (see Fig. S1 for structure details) are gaining a lot of

† Equally contributed to the work reported.

attention these days due to a considerable degree to their outstanding luminescence properties. Indeed, these complexes demonstrate bright red/near-infrared emission which is characterized by high quantum yields and microsecond lifetimes under ultraviolet [1] and X-ray irradiation [2]. Recently, the $[\{Mo_6I_8\}L_6]^{2-}$ cluster complexes, where L are residues of some strong acids such as, for example, $C_nF_{2n+1}COO^-$ (n = 1, 2, 3), OTs^- (p-toluenesulfonate) or NO_3^-, were shown to demonstrate the record values of the photoluminescence quantum yields (up to ~0.8) and lifetimes (up to ~360 μs) among all known transition metal cluster complexes [3-7]. Furthermore, the bright red/near-infrared luminescence produced by such cluster complexes is able to generate singlet oxygen [8-12] that can be used, for example, in photodynamic cancer therapy [13, 14]. The high quantum yields and ability to generate singlet oxygen make molybdenum cluster complexes attractive for biological and medical applications as bioimaging and biolabeling agents as well [15].

Though octahedral molybdenum cluster complexes possess such intriguing properties, the majority of the known $\{Mo_6X_8\}^{4+}$-based cluster compounds are insoluble in water and/or potentially react with physiological environments [16-18]. This circumstance doesn't allow them to be used in biological and medical applications. Recently, it was demonstrated that similar octahedral metal-cluster complexes could be either surrounded by specific biocompatible moieties [19-22], or encapsulated in bioinert matrices, *e.g.* organic polymers [3, 23-27], dendrimers [28] or inorganic oxides [8, 29-34] or metal-organic frameworks (MOFs) [35-38] that can prevent a chemical interaction with physiological media of these cluster complexes.

The first outline of the concept of using MOF materials for drug delivery was made by G. Férey in 2006 [39, 40]. Therein, authors have exposed for the first time the remarkable capability of porous metal-organic frameworks for drug hosting and controlled delivery, with the chromium terephthalate metal-organic framework, MIL-100 and MIL-101 (MIL, Matérial Institut Lavoisier) acting as porous matrices and ibuprofen as a model substance. Later the different MOFs for delivery of various drugs were observed [41-46]. However, the applicability of MOFs is not limited by the "simple" encapsulation of small drug molecules with the following release of the loaded substances in physiological media. Some MOFs demonstrated inherent biological activity [47]. Another approach to biological active material is a post-synthetic modification of MOFs [45].

In this contribution, we report the preparation of new inclusion compounds combining a $\{Mo_6I_8\}^{4+}$-based cluster complex and the nanosized metal-organic framework MIL-101 using two alternative approaches, namely the direct introduction of the hexamolybdenum cluster complex into MIL-101 and the introduction of the cluster complex into preliminary modified MIL-101 (the post-synthetic modification approach). The molybdenum cluster complex possesses luminescence

properties and ability for singlet oxygen generation whereas chromium(III) oxoterephthalate MIL-101 is a good candidate as storage matrix due to its outstanding stability and mesoporosity (see Fig. S2). Delivery of the inclusion compounds into Hep-2 cells and their photodynamic properties were also considered.

2 Material and methods

2.1 Synthesis section

All reagents and solvents employed were commercially available and used as received without further purification. Pyrazine (≥99%) (pyz) was purchased from Sigma-Aldrich. The cluster compound $(Bu_4N)_2[\{Mo_6I_8\}(NO_3)_6]$ was obtained according to the procedure described [25].

2.1.1 Synthesis of MIL-101

Nanosized MIL-101 was synthesized according to the slightly modified procedure [48]. In a typical synthesis, chromium nitrate (1.2 g, 3 mmol), terephthalic acid (500 mg, 3 mmol), 3 M HF (1 mL, 3 mmol), and H_2O (15 mL) were mixed in a Teflon lined autoclave, heated up to 220 °C in 3 h and kept at this temperature for 6 h. Then mixture was cooled down to the room temperature. The solid obtained was filtered off using a glass filter with the pore size 160 μm to remove crystals of excess terephthalic acid and then through a fine paper filter. The purification of the crude MIL-101 product was carried out in four steps: double treatment with N,N-dimethylformamide (DMF) at 60 °C during 1 h per each treatment and then double treatment with hot ethanol at 70 °C during 3 h per each treatment. The resulting material was finally dried overnight at 80 °C.

*2.1.2 Synthesis of {Mo_6I_8}@MIL-101 (**1**)*

Cluster complex $(Bu_4N)_2[\{Mo_6I_8\}(NO_3)_6]$ (50 mg, 0.020 mmol) was dissolved in 4 mL of CH_2Cl_2 and MIL-101 (300 mg, ~0.3 mmol) was added. The mixture obtained was stirred for 30 min at room temperature. After impregnation the solid product **1** was filtered off, washed with two portions of CH_2Cl_2 (2×500 μL) and dried in air at 70 °C. The yield of **1** was 330 mg.

IR, ν/cm^{-1}: 3100 (med, brd), 1698 (sh), 1654 (str), 1614 (str), 1550 (sh), 1506 (med), 1433 (sh), 1400 (str), 1292 (med), 1157 (wk), 1105 (wk), 1018 (wk), 926 (wk), 881 (wk), 829 (wk), 808 (wk), 777 (wk), 746 (med), 704 (wk), 663 (wk), 577 (med).

Chemical analysis: Mo/Cr = 1/8.37.

*2.1.3 Synthesis of MIL-101-pyz (**2**)*

MIL-101 (500 mg, ~0.5 mmol) was activated in dynamic vacuum during 6 h at 180 °C for complete removal of water (the residual pressure was $5 \cdot 10^{-2}$ mbar). After that MIL-101 was introduced to the toluene solution of pyrazine (pyz, 84 mg, 1.05 mmol) in 10 mL of toluene under the Ar flow. After stirring for 6 h at 80 ºC, and then 2 d at room temperature the solid product **2** was filtered off, washed with two portions of toluene (2×5 mL) and dried in air at 70 °C. The yield of **2** was 270 mg. Anal. Calcd for $Cr_3OF(C_8H_4O_4)_3(C_4H_4N_2)_{1,7}(H_2O)_6$ ($C_{30.8}H_{30.8}Cr_3FN_{3.4}O_{19}$): C, 39.9; H, 3.3; N, 5.1. Found: C, 39.9; H, 3.3; N, 5.1.

IR, ν/cm^{-1}: 3100 (med, brd), 1701 (med), 1655 (str), 1612 (str), 1549 (str), 1506 (str), 1433 (sh), 1400 (str), 1319 (med), 1294 (med), 1254 (med), 1157 (med), 1124 (sh), 1105 (med), 1057 (wk), 1018 (med), 924 (wk), 881 (wk), 827 (med), 808 (med), 746 (str), 704 (str), 663 (med), 579 (str), 463 (med).

*2.1.4 Synthesis of {Mo_6I_8}-MIL-101-pyz (**3**)*

Cluster complex $(Bu_4N)_2[\{Mo_6I_8\}(NO_3)_6]$ (50 mg, 0.020 mmol) was dissolved in CH_2Cl_2 (4 mL) and **2** (150 mg, ~0.16 mmol) was added. The obtained mixture was stirred for 30 min at room temperature. After the reaction the solid product **3** was filtered off, washed with two portions of CH_2Cl_2 (2×500 μL) and dried in air at 70 °C. The yield of **3** was 170 mg.

IR, ν/cm^{-1}: 3428 (str, brd), 1695 (sh), 1670 (sh), 1624 (str), 1549 (med), 1508 (med), 1400 (str), 1159 (wk), 1109 (wk), 1059 (wk), 1016 (wk), 883 (wk), 831 (wk), 748 (str), 665 (med), 588 (str).

Chemical analysis: Mo/Cr = 1/3.83

*2.2 Extraction of cluster units from **1** and **3***

3 mg of **1** and **3** were placed in a glass vial of 10 mL and saline (3 mL) was added. The mixtures were then left for 24 h. As blank experiments, the MIL-101 and **2** were also placed in the similar experimental conditions. After extraction, the reaction mixtures were centrifuged (RCF 22000×g) and decanted. The supernatant **1** of yellow color was then investigated by Electrospray Ionization Mass Spectrometry (ESI-MS). As a reference sample for ESI mass spectrometry the solution obtained by hydrolysis of 40 mg of $(Bu_4N)_2[\{Mo_6I_8\}(NO_3)_6]$ in 30 mL of distilled water was used.

2.3 Analytical methods

2.3.1 Chemical analysis

Elemental analysis on C, H, N was carried out using Euro Vector EA3000.

Chromium and molybdenum content was determined by ICP-AES technique (Inductively Coupled Plasma Atomic Emission Spectroscopy) using iCAP 600 apparatus. Before the analyses the samples (*ca.* 20 mg) were digested in *ca.* 10 mL of an aqueous solution of potassium hydroxide (*ca.* 150 mg) and hydrogen peroxide (0.5 mL, 30%).

2.3.2 Powder X-ray diffraction (XRD)

XRD patters were collected on Shimadzu XRD 7000S diffractometer with $\lambda_{Cu}(K_{\alpha1}, K_{\alpha2})$ = 1.54059, 1.54439 Å, with the step of 0.03°/sec in the range of 2θ angles from 3° to 35°.

2.3.3 Thermogravimetric analysis

The thermogravimetric analysis was performed on NETZSCH TG 209 F1 Iris Thermo Microbalance. Approximately 10 mg of each sample were placed on an aluminum sample holder and heated from room temperature up to 700 °C with the rate of 10 °C·min^{-1} in a helium atmosphere.

2.3.4 Surface area and porous structure

Nitrogen adsorption measurements at 77 K were carried out using Autosorb iQ (Quantachrome Instruments). The samples were preliminary degassed in dynamic vacuum at 450 K for 20 hours. N_2 adsorption-desorption isotherms were measured within the range of relative pressures p/p_0 from 10^{-4} to 0.99. The specific surface area was calculated from the data obtained based on Brunauer-Emmet-Teller and Langmuir models. The Gourvich and Saito&Foley approaches, as the most appropriated for the studied materials, were employed to estimate the total pore volume and the pore size distribution, respectively.

2.3.5 Size and morphology

High Resolution Transmission Electron Microscopy (HRTEM) images were made with a JEM-2200FS (JEOL) microscope with a lattice-fringe resolution of 0.1 nm at an accelerating voltage of 200 kV. Suspensions in isopropanol were deposited on carbonfilm-coated copper grids.

2.3.6 ESI Mass-spectrometry

The mass spectrometric (MS) detection was performed with direct injection of liquid samples via automatic syringe pump KDS 100 (KD scientific, USA) at 180 µL/h rate on an electrospray ionization quadrupole time-of-filght (ESI-q-TOF) high-resolution mass spectrometer Maxis 4G (Bruker Daltonics, Germany). Mass spectra were recorded in both positive and negative modes with 300–3000 m/z range. The instrument parameters were: end plate offset 500 V; capillary voltage

−4200 V for positive mode, +2800 V for negative mode; nebulizer pressure 1 bar; dry gas flow 4 L/min; dry gas temperature 180 °C. The MS calibration was performed with ESI-L calibration mix (Agilent, USA); typical resolution was *ca.* 50000, accuracy <1 ppm.

2.3.7 Singlet Oxygen Generation

The singlet oxygen generation was investigated as described previously [49, 50]. In a typical experiment 10 mg of MIL-101, **1**, **2** or **3** and the solution of 29 mg (0.12 mmol) of 2,3-diphenyl-*para*-dioxene in acetone-d_6 (0.6 mL) were placed in a conventional NMR tube. After that, the mixture was saturated with oxygen for 5 min. The sealed tube was then irradiated by DRSh-500 mercury lamp with a filtered light ($\lambda \geq 400$ nm). Then ^{1}H NMR (200 MHz) spectra were collected on a Bruker Avance 200 NMR spectrometer.

2.3.8 Luminescence properties

For emission measurements, the powdered samples were placed between two non-fluorescent glass plates. The absorbance of an aqueous solution of hydrolyzed $(Bu_4N)_2[\{Mo_6I_8(NO_3)_6\}]$ was set < 0.1 at 355 nm. The solution was poured into two quartz cuvettes and one of them was deaerated by purging with an Ar-gas stream for 30 min and then the cuvette was sealed. Measurements were carried out at 298 K. The samples were excited by 355-nm laser pulses (6 ns duration, LOTIS TII, LS-2137/3). Corrected emission spectra were recorded on a red-light-sensitive multichannel photodetector (Hamamatsu Photonics, PMA-12). For emission decay measurements, the emission was analyzed by a streakscope system (Hamamatsu Photonics, C4334 and C5094). The emission quantum yields were determined by an Absolute Photo-Luminescence Quantum Yield Measurement System (Hamamatsu Photonics, C9920-03), which comprised an excitation Xenon light source (the excitation wavelength was set at 380 nm), an integrating sphere, and a red-sensitive multichannel photodetector (Hamamatsu Photonics, PMA-12).

2.4 Biological methods

2.4.1 Cell Culture

Human larynx carcinoma cell line (Hep-2) was purchased from the State Research Center of Virology and Biotechnology VECTOR and cultured in Eagle's Minimum Essential Medium (EMEM, pH = 7.4) supplemented with a 10% fetal bovine serum under a humidified atmosphere (5% CO_2 plus 95% air) at 37 °C.

2.4.2 MTT-assay

The effect of the MIL-101, **1**, **2** and **3** on the cells metabolic activity was determined using the 3-[4,5-dimethylthiazol-2-yl]-2,5-diphenyl tetrazolium bromide (MTT) colorimetric assay. The Hep-2 cells were seeded into 96-well plates at $5 \cdot 10^3$ cells/well in a medium containing MIL-101, **1**, **2** or **3** with concentrations from 500 to 0.5 μg/mL and then incubated for 72 h under 5% CO_2 atmosphere. Fresh culture medium was added to control cells. After that 5 μL of the MTT solution with the concentration of 5 mg/mL was added to each well, and the plates were incubated for 4 h and then solubilized with a dimethyl sulfoxide solution, as indicated in the manufacturer's instructions. The optical density was measured with a plate reader Multiskan FC (Thermo scientific, USA) at the wavelength of 620 nm. The experiment was repeated three times on the separate days.

2.4.3 Confocal Laser Scanning Microscopy (CLSM)

Hep-2 cells were seeded on slides ($1.5 \cdot 10^5$ cells/slide) and incubated overnight at 37 °C under 5% CO_2 atmosphere. The medium was then replaced with a fresh medium containing 62.5 μg/mL of MIL-101, **1**, **2** or **3** and incubated for 24 h. The cells incubated in the absence of investigated compounds were also used as a control. Finally, the cells were washed twice with phosphate buffer saline, fixed in 4% paraformaldehyde and visualized by using a Zeiss LSM 510 confocal microscope (Carl Zeiss Inc., Jena, Germany) equipped with a laser diode (405 nm) for fluorescence and with a 100× oil immersion objective. The images were obtained and analyzed with ZEN 2009 software.

*2.4.4 Detection and quantification of ROS levels induced by {Mo_6I_8}@MIL-101 (**1**) on Hep-2 cells*

Hep-2 cells were seeded in 96-well plate (1×10^4 cells/well) and incubated overnight at 37 °C under 5% CO_2 atmosphere. The medium was then replaced with a fresh medium containing 125, 62.5 and 31.25 μg/mL of **1** and incubated for 24 h. The cells incubated in free media and with 100 μM H_2O_2 were used as a negative and positive control respectively. The cells were pre-incubated with 10 μM 5,6-carboxy-2',7'-dichlorofluoresceindiacetate (DCFH-DA) (Sigma-Aldrich) in HEPES (4-(2-hydroxyethyl)-1-piperazineethanesulfonic acid) for 5 min at 37 °C and then were irradiated with 500 W halogen lamp ($\lambda \geq 400$ nm) for 15 min. Cell nucleus were stained by Hoechst 33342 IN Cell Analyzer 2200 (GE Healthcare, UK) was used to perform automatic imaging of four fields per well under 200X magnification, in fluorescence channels. The images produced were used to analyse DCFH-DA fluorescent intensity of positive cells among the whole

population using the IN Cell Investigator software (GE Healthcare, UK). Data represent the mean DCFH-DA fluorescence intensity.

*2.4.5 Photodynamic treatment by {Mo_6I_8}@MIL-101 (**1**) and {Mo_6I_8}-MIL-101-pyz (**3**) of Hep-2 cells*

The Hep-2 cells were seeded in 96-well plates at the density of 5×10^3 cells/well and cultured for 24 h. The medium was then replaced with the fresh medium containing from 500 to 125 μg/mL of {Mo_6I_8}@MIL-101 (**1**) and {Mo_6I_8}-MIL-101-pyz (**3**) incubated for 24 h and then were irradiated with 500 W halogen lamp (λ ≥400 nm) for 30 min to apply a total light dose 20 J/cm^2. Cells cultured in the medium without **1** served as a negative control. The viability of treated and control cells was assayed and analysed 4 h Hoechst/Propidium iodide (PI) staining as previously described by Lee et al [51]. The irradiated cells and control cells were stained with Hoechst 33342 (Sigma-Aldrich) for 30 min at 37 °C and PI (Sigma-Aldrich) for 10 min at 37 °C. IN Cell Analyzer 2200 (GE Healthcare, UK) was used to perform automatic imaging of six fields per well under 100X magnification, in brightfield and fluorescence channels. The images produced were used to analyse live, apoptotic and dead cells among the whole population using the IN Cell Investigator software (GE Healthcare, UK).

3 Results and discussion

3.1 Materials preparation and characterization

Highly emissive and photodynamically active $\{Mo_6I_8\}^{4+}$-based cluster complexes have a good potential as a luminescence probe or photosensitizer in biomedical applications such as bioimaging or photodynamic therapy, respectively. However, the low hydrolytic stability of such complexes leading to the formation of poorly soluble derivatives in aqueous solutions and therefore in physiological liquids limits their use in biomedicine. There are several approaches to prevent the undesirable hydrolysis of a soluble complexes $[\{Mo_6I_8\}L_6]^{2-}$. It is possible to introduce them into matrices of different nature: organic polymers [3, 23-25], inorganic porous solids such as silicon dioxide [8, 29, 30, 33, 34] or metal-organic frameworks [36, 37].

The encapsulation of $[\{Mo_6I_8\}(NO_3)_6]^{2-}$ into nanosized MIL-101 led to the formation of inclusion compound **1** with "host-guest" interaction type. Recently, the encapsulation of different cluster complexes of molybdenum and rhenium, namely $(Bu_4N)_2[\{Mo_6Br_8\}F_6]$, $(Et_4N)_2[\{Mo_6Cl_8\}Cl_6]$, $(Bu_4N)_4[\{Re_6S_8\}(CN)_6]$, $K_4[\{Re_6S_8\}(HCOO)_6]$ and $K_4[\{Re_4S_4\}F_{12}]$ into MIL-101 matrix was demonstrated [35-38, 52]. It was shown that such anionic clusters readily

penetrate into the cages through large windows (10–15 Å) and interact strongly with the matrix due to the positive electrical charge of the MIL-101 framework. The elemental analysis of the compound **1** showed the ratio of Cr/Mo = 8.37 that corresponded to 0.06 clusters per formula unit of MIL-101 or *ca.* 0.7 clusters per each mesocage of the framework.

Inclusion of cluster complexes into MOFs occurs readily as well as, unfortunately, their leaching outside from the pores. We have suggested a novel approach to anchor cluster complexes inside a MOF-matrix by using an additional ditopic ligand. To demonstrate the validity of such idea, mesoporous chromium terephthalate MIL-101 and its pyrazine-modified derivative MIL-101-pyz [53] were used for hexamolybdenum cluster inclusion.

In our present work, pyrazine-modified framework MIL-101-pyz (**2**) was used for covalent binding of the hexamolybdenum cluster complex *via* N atom of the ditopic pyrazine ligand. The introduction of $[\{Mo_6I_8\}(NO_3)_6]^{2-}$ into **2** led to the formation of compound **3** with the covalent bond between the cluster unit and framework. Such type of connectivity is performed due to the high lability of terminal NO_3^--ligands of the cluster complex that are substituted by the pyrazine groups presented in **2**. Earlier, the complexes $[\{Mo_6X_8\}(NO_3)_6]^{2-}$ (X = Cl, Br or I) were used as precursors for preparation of hybrid materials with the general formula $\{Mo_6X_8\}$@PS-SH (PS-SH is thiol-containing polystyrene microspheres) by the treatment of PS-SH with the corresponding cluster complex. It resulted in the substitution of six NO_3^--ligands by thiol groups of the polymer matrix [23, 25]. Here we demonstrate a similar approach with substitution of NO_3^--ligands by nitrogen atom of pyrazine bound to MIL-101. The elemental analysis of **3** showed the ratio of Cr/Mo = 3.83 that is corresponded to 0.13 cluster units per formula unit of MIL-101-pyz or 1.47 clusters per mesocage of the framework.

The shape and the morphology of the starting MIL-101 prepared here were characterized *via* TEM (Fig. S3). The electron microscope image showed that the compound is a crystalline powder with the crystal size of about 100-200 nm. Powder XRD patterns of MIL-101 and synthesized compounds **1**–**3** are shown in Fig. S4. The powder XRD data confirmed that all modifications of MIL-101 (cluster complex inclusion and covalent modification with pyrazine) did not affect the structure of the framework.

High porosity of the compounds obtained was established by nitrogen cryoadsorption. Textural parameters of MIL-101 and samples **1**–**3,** adsorption–desorption isotherms at 77 K are presented in Supplementary Information (Table S1, Fig. S5). Compounds **1**–**3** are highly porous, nevertheless compounds **1–3** demonstrate lower nitrogen adsorption capacity, total pore volume and surface area

compared with the starting MIL-101. Such changes in adsorption behavior are due to partial occupying of inner free volume of MIL-101 by cluster complexes and pyrazine molecules and higher density of the material. Thus, the compounds obtained keep the porous structure of pristine MIL-101 along with a slight decrease in pore volumes and pore widths (Fig. S6).

3.2 Stability of the cluster doped materials in water

To prove the strong binding of the cluster units by MIL-101-pyz (**2**) the additional experiments were carried out. The compounds **1** and **3** were placed in physiological saline and left for 24 h. As blank experiments, the MIL-101 and **2** were also kept under the same experimental conditions. After the extraction and the following centrifugation it was observed that the supernatant in case of the compound **1** was colored (Fig. 1). In contrast, in the case of compound **3**, the supernatant was almost colorless, visually confirming the strong binding of cluster units and MIL-101 framework *via* ditopic pyrazine ligand by means of a bond "N atom of pyrazine molecule – $\{Mo_6I_8\}$-unit".

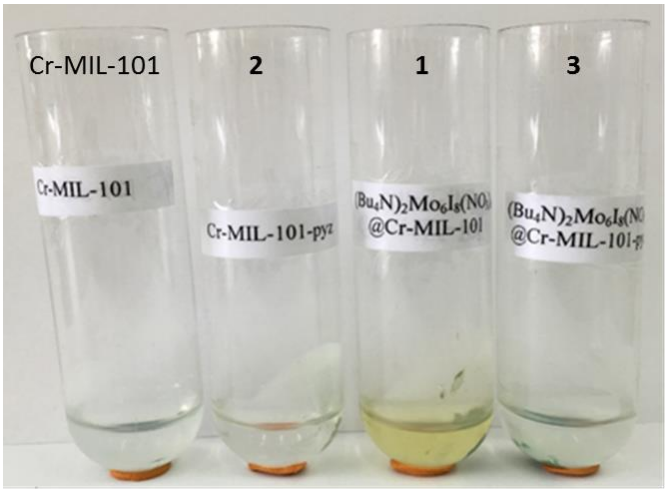

Fig. 1. Aqueous supernatants MIL-101, **1**, **2** and **3** after extraction. Supernatant **1** is yellow.

The yellow supernatant **1** was then investigated by ESI mass-spectrometry. The mass spectrum obtained was absolutely the same as the spectrum of hydrolyzed $[\{Mo_6I_8\}(NO_3)_6]^{2-}$ (Fig. S7a). The hydrolysis of $[\{Mo_6I_8\}(NO_3)_6]^{2-}$ cluster complex in distilled water resulted in the formation of different cluster ions, as it was confirmed by ESI mass-spectrometry of the resultant solution. Thus, in the region of m/z from 810 to 900 (positive mode) a set of signals with complicated structure was observed (Fig. S7b). Detailed analysis of the spectrum showed the presence of a number of cluster ions, resulted from the substitution of the terminal NO_3^- ligands. The spectrum is in a good agreement with simulation (Fig. S7b and Fig. S8), which is the sum of peaks corresponding to different cationic units, namely $(\{Mo_6I_8\}(OH)_2{\cdot}xH_2O)^{2+}$ and $(\{Mo_6I_8\}(OH)(NO_3){\cdot}yH_2O)^{2+}$ (where x = 1–9 and y = 0–6). However, the increase of pH to the physiological value of 7.4 led to the

precipitation of the poorly water-soluble neutral aquahydroxo complex $[\{Mo_6I_8\}(H_2O)_2(OH)_4]\cdot zH_2O$ accompanied by the bleaching of solution (Fig. S9) [29].

3.3 Photophysical studies

3.3.1 Luminescence properties

Luminescence from the powdered samples of the starting MIL-101, compounds **1** and **3** as well as from hydrolyzed $[\{Mo_6I_8\}(NO_3)_6]^{2-}$ in both aerated and deaerated aqueous solutions was studied. The emission spectra are shown in Figs. 2 and S10, and the emission maximum wavelengths (λ_{em}), quantum yields (Φ_{em}), and lifetimes (τ_{em}) are summarized in Table 1. Despite the fact that the red photoluminescence of the samples can be easily observed by a naked eye, photoluminescence quantum yield values are too low to be properly determined using the integrating sphere, *i.e.*, are less than 0.01.

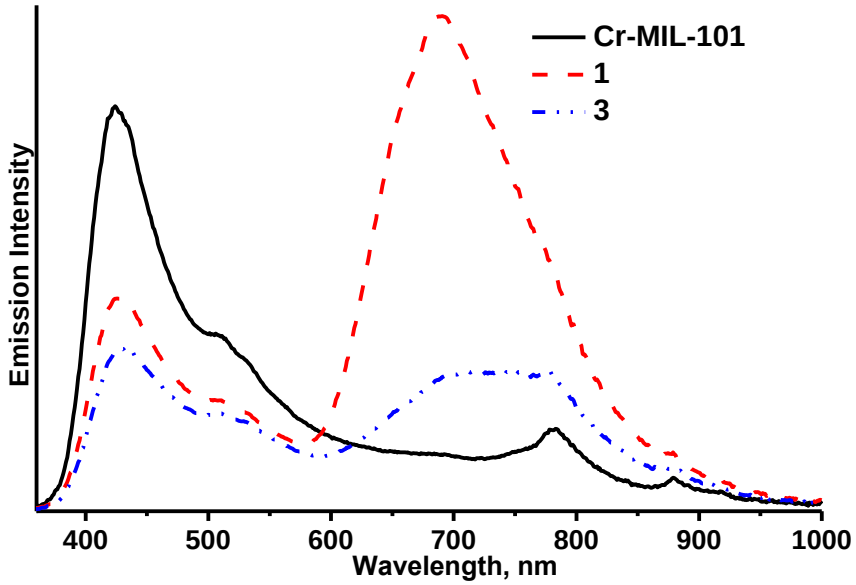

Fig. 2. Corrected luminescence spectra of MIL-101 and hybrid compounds **1** and **3**. Spectra were recorded under identical experimental conditions.

In the spectra, two peaks with the maximum (λ_{em}) at ~430 nm and ~780 nm were observed. These peaks can be attributed to the ligand-to-metal charge transfer (430 nm) [54-56] and the transition $^2E \rightarrow {}^4A_2$ in the Cr^{III} atoms (780 nm) [36, 57]. Broad luminescence peak with the maximum at ~700 nm for **1** and **3** definitely referred to the molybdenum cluster complex incorporated into the MOF. However, the "cluster" emission intensity for **3** was much lower than that for **1**. The difference in the emission intensity (Fig. 2) as well as in emission lifetimes (Table 1) between **1** and **3** can be explained by different outer ligand environment of the loaded cluster complex $[\{Mo_6I_8\}(NO_3)_6]^{2-}$ due to the substitution of terminal NO_3^--ligands by pyrazine molecules

coordinated to Cr atoms in **2**. Similar decrease in the "cluster" emission intensity was previously observed after internalization of $[\{Mo_6I_8\}(NO_3)_6]^{2-}$ into PS-SH that was also accompanied by NO_3^- -ligand substitution [23, 25]. On the other hand, coordination of $\{Mo_6I_8\}^{4+}$ cluster units by conjugated pyrazine ligands led to the formation of the alternative energy dissipation pathway "cluster nucleus → conjugated ditopic ligand → metal-organic framework". Such pathway was previously demonstrated by the similar decrease in the luminescence intensity of MIL-101-bipy impregnated by the solution of $[\{Re_6S_8\}(HCOO)_6]^{4-}$ in comparison with $[\{Re_6S_8\}(HCOO)_6]^{4-}$@MIL-101 [35]. Also it should be kept in mind that both luminescence lifetimes and quantum yields quite strongly depend on oxygen presence. Thus, a deaerated aqueous solution of the hydrolyzed complex $[\{Mo_6I_8\}(NO_3)_6]^{2-}$ was characterized by about 7 times longer emission lifetime and one order of magnitude higher quantum yield than the aerated solution (Fig. S10, Table 1).

Table 1. Photophysical parameters of samples studied.

Sample	λ_{em} / nm	τ_{em} / μs (A)	Φ_{em}
Solid samples			
MIL-101	424, 783	τ_1 = 2.75 (0.01) τ_2 = 0.48 (0.08) τ_3 = 0.08 (0.91)	<0.01
1	424, 690	τ_1 = 14.3 (0.02) τ_2 = 0.88 (0.19) τ_3 = 0.16 (0.79)	<0.01
3	431, 740	τ_1 = 7.28 (0.02) τ_2 = 1.36 (0.19) τ_3 = 0.25 (0.79)	<0.01
Aqueous solutions			
hydrolyzed $(Bu_4N)_2[\{Mo_6I_8\}(NO_3)_6]$, aerated	700	8.16	0.02
hydrolyzed $(Bu_4N)_2[\{Mo_6I_8\}(NO_3)_6]$, deaerated	700	55.3	0.11

3.3.2 Singlet oxygen generation

As it was demonstrated in Table 1 and in some previous papers, the photophysical parameters of hexamolybdenum cluster complexes in solutions, emission lifetimes and quantum yields in particular are very sensitive to the presence of molecular oxygen [3, 6, 24, 58, 59]. One of the reasons of such emission quenching is the energy transfer from the excited cluster complex to triplet oxygen ($^3O_2$) resulting in the generation of singlet oxygen ($^1O_2$) [11, 60]. Since the compounds **1** and **3** are porous enough for molecular oxygen penetration, the investigation of singlet oxygen generation ability was carried out (Fig. S11). The compound 2,3-diphenyl-*para*-dioxene is well-established as a singlet oxygen trap, being easily oxidized by the singlet oxygen to form ethylene

glycol dibenzoate (Scheme S1). The calculated conversions of 2,3-diphenyl-*para*-dioxene after photoirradiation by light with $\lambda \geq 400$ nm are given in Table 2 and Fig. S12.

Table 2. Singlet oxygen generation under visible light irradiation ($\lambda \geq 400$ nm)

Sample	**Conversion of 2,3-diphenyl-para-dioxene / %**		
	1 h	3 h	5 h
MIL-101	0.1	0.5	0.5
1	1.0	2.4	5.8
2	0	1.1	1.2
3	0.3	1.9	5.4

Cluster containing compounds **1** and **3** demonstrate satisfactory activity in the singlet oxygen generation, whereas for MIL-101 as well as for its pyrazine derivative **2** only negligible conversion of 2,3-diphenyl-*para*-dioxene was observed. Moreover, the singlet oxygen generation activity is comparable for both **1** and **3** in spite of two times higher cluster content in **3** than in **1**. Nevertheless, the activities in the singlet oxygen generation of MIL-101 based inclusion compounds are higher than those recently estimated for hexamolybdenum cluster-doped silica microparticles of 500 nm [29].

3.4 Biological properties

3.4.1 Cytotoxicity on Hep-2 cells

The toxicity of compounds plays crucial role for their implementation in photodynamic therapy and other bioapplications. Chromium containing compounds have an especial issue due to a very high Cr^{VI} toxicity. In our investigation we use the quite stable compound MIL-101 containing Cr^{III} which toxicity is much less than Cr^{VI}. Even so, we evaluated the influence of MIL-101, **1**, **2** and **3** on the metabolic activity of Hep-2 cells using the MTT-assay. The yellow tetrazolium MTT (3-(4,5-dimethylthiazolyl-2)-2,5-diphenyltetrazolium bromide) is reduced by metabolically active cells, namely because of dehydrogenase enzymes' activity. The resulting intracellular purple formazan can be solubilized and quantified by means of spectrophotometry. The rates of metabolically active cells were determined against the negative control. We showed that the concentrations of **1** and MIL-101 from 0.5 μg/mL to 125 μg/mL did not affect viability of the cells, *i. e.* the cells viability was more than 80 %. The half maximal inhibitory concentrations (IC_{50}) of MIL-101 and **1** for cells were estimated to be 744±16 μg/mL and 535±48 μg/ml respectively. Compounds **2** and **3** had stronger effect on the metabolic activity of cells. For example, the cell viability after treatment by **2** and **3** was less than 80 % in the same range of the concentrations up to 125 μg/ml, suggesting that

the concentrations of **2** and **3** less than 62.5 μg/ml were allowed for further biological applications. IC_{50} of **2** and **3** for the cells were equal to 407±26 μg/mL and 339±16 μg/mL, respectively (Fig. 3). Thus, the results obtained on the influence of MIL-101 and its derivatives on Hep-2 viability showed that the pristine MIL-101 and its inclusion compounds with the hexamolybdenum cluster complexes have a low cytotoxicity. Furthermore, the pyrazine free compounds MIL-101 and **1** have lower cytotoxicity than their pyrazine containing counterparts.

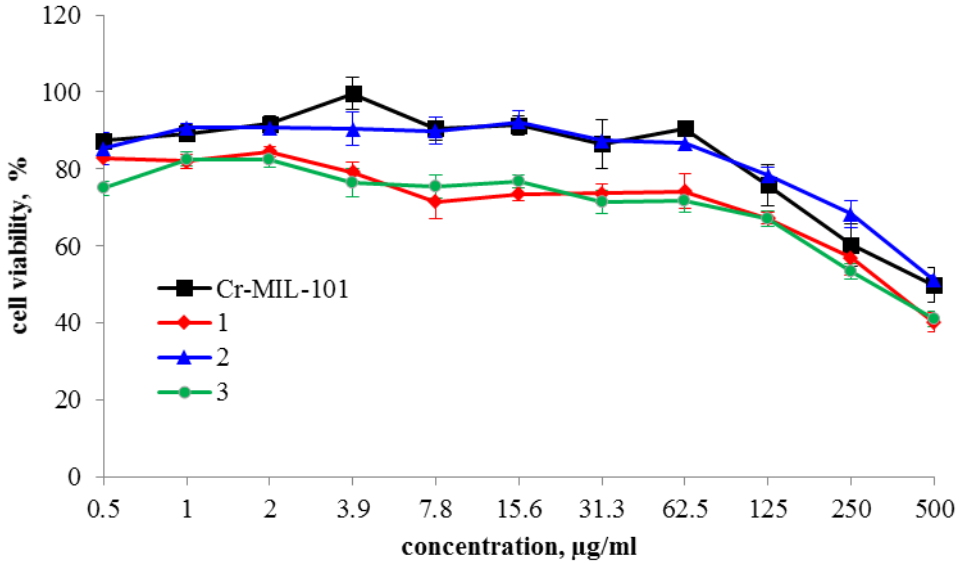

Fig. 3. Effect of MIL-101 and its derivatives with hexamolybdenum cluster complexes and pyrazine **1**–**3** on viability of Hep-2 cells measured by MTT.

3.4.2 Confocal microscopy

To assess the ability of MIL-101 and compounds **1**–**3** to internalize into cells, confocal fluorescence microscopy of the Hep-2 cells after combined incubation with the medium containing 62.5 μg/mL MIL-101, **1**, **2** or **3** was carried out. The images obtained (Fig. 4) have demonstrated, that MIL-101 and **1**–**3** adhered to cell membrane and did not penetrate into the intracellular space. Pyrazine derivatives showed stronger ability to adhere to the surface of the cell membrane in comparison with the pristine MIL-101. After cell incubation with **1** it was observed that the cytoplasm of cells displayed diffuse red fluorescence, which was indicative of the penetration of the fluorescent substance inside the cells. Since the distribution of red fluorescence within the cytoplasm was uniform, the cluster complexes included in **1** presumably came out of the framework and diffused through the cell membrane into the cytoplasm (Fig. 4). It clearly indicated the auxiliary effect of MIL-101 matrix which provided delivery of the cluster complexes up to the cell membrane without leaching and dissipation, whereupon the cluster complexes could penetrate into the cytoplasm.

On the contrary, cell incubation with **3** led only to the red luminescence from external cell surfaces due to the impossibility of the penetration of MIL-101 through the cell membrane as well as strong bonding of the cluster complexes through pyrazine moieties with metal-organic framework. Thus, in this case the penetration of the cluster complexes into cellular space did not occur.

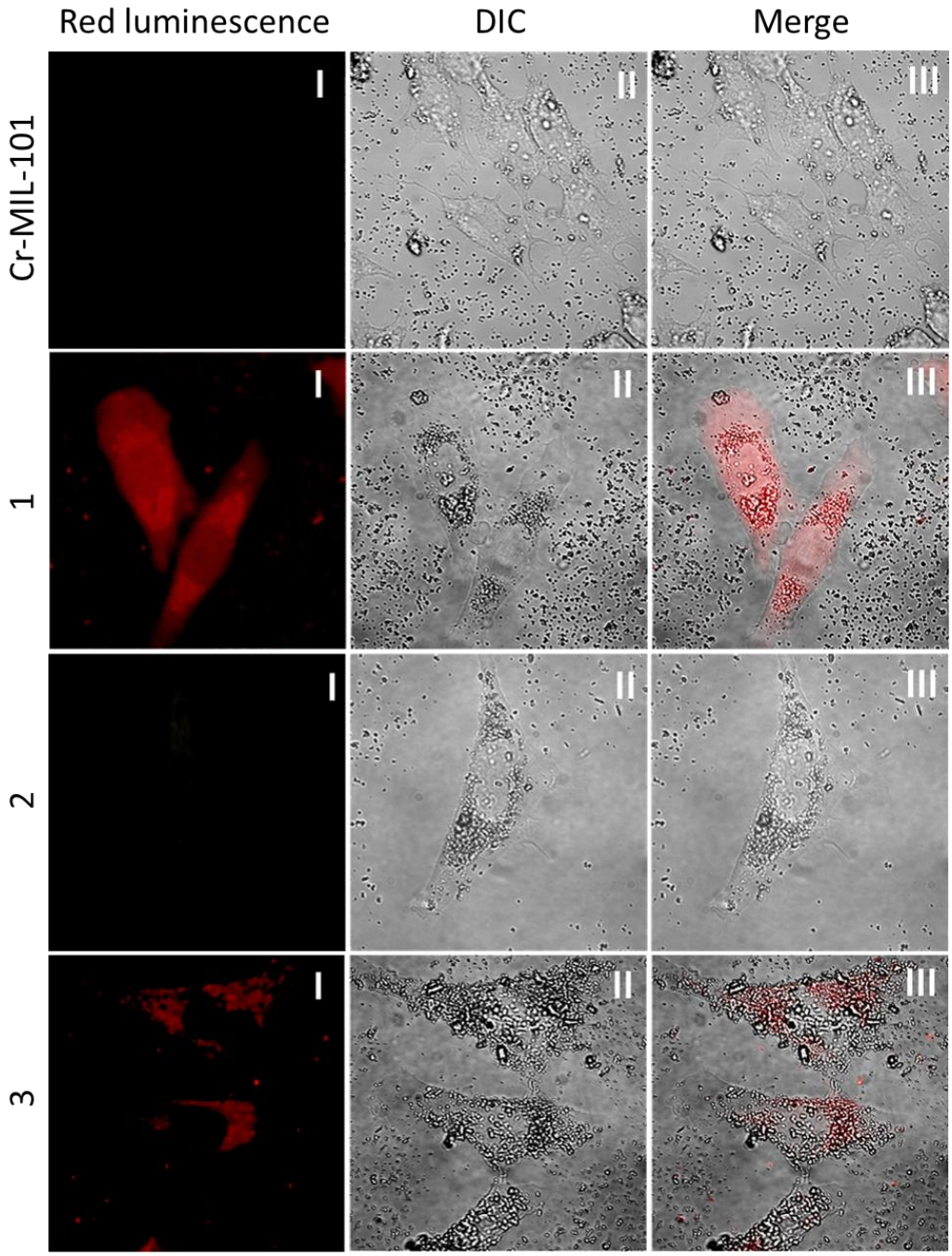

Fig. 4. Cellular uptake of cluster complexes after incubation of Hep-2 cells with MIL-101, **1**, **2** or **3** visualized by confocal fluorescence microscopy: red fluorescence (I), differential interference contrast (II) and merged images (III). Magnification is X100.

3.4.3 Reactive oxygen species generation in living cells

As it was shown above, the hexamolybdenum cluster-doped MIL-101 materials are able to generate singlet oxygen. Since photodynamic therapy (PDT) is based on the generation of different reactive oxygen species (ROS) such as singlet oxygen $^1O_2$, which is widely considered to be the main cytotoxic agent in PDT damaging and inducing apoptosis of tumor cells, the next stage of this study was to determine and quantify the ROS level inside Hep-2 cells induced by **1**. To monitor the presence of intracellular ROS, we used cell-permeable fluorescent probe 5,6-carboxy-2',7'-dichlorofluoresceindiacetate (DCFH-DA) sensitive to oxidation by different ROS including singlet oxygen. The cells incubated in free media and with H_2O_2 as irradiation-independent ROS were used as a negative and positive control, respectively. The fluorescence of DCFH-DA and corresponding ROS level are high and do not depend on light in the presence of H_2O_2 (Fig. S13) whereas the ROS level in the cells incubated in free media is negligible both before and after irradiation. The cells incubated in the presence of compound **1** have demonstrated bright green fluorescence after photoirradiation which is clearly indicated about high ROS level (Fig. S14). As it is shown in Fig. 5 the ROS level increase in a concentration-dependent manner upon photoirradiation, whereas the level of fluorescent intensity before photoirradiation was several times lower. Thus, these data confirmed that **1** is not only able to generate ROS *in vitro* (See *3.2.2*), but also in the living cells.

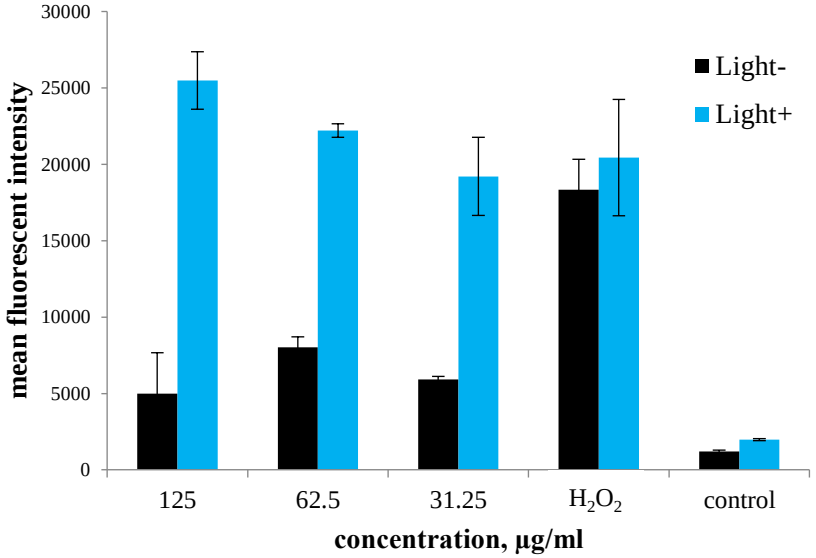

Fig. 5. Detection and quantification of ROS levels induced by **1** on Hep-2 cells before (blue columns) and after (red columns) photoirradiation, respectively. Data represent the mean DCF fluorescence intensity.

3.4.4 Photodynamic treatment on Hep-2 cells

We have established that hexamolybdenum clusters included in MIL-101 can come out of the framework and diffuse through the Hep-2 cell membrane into the cytoplasm (Fig. 4)

where they possess ROS generation ability (Fig. 5). Both these factors play a crucial role in employing compound **1** as a tool for intracellular photosensitisation. Compound **3** could be used as a negative control, because it strongly bonded to MIL-101 and cannot penetrate into the cells. Hep-2 cells were treated by compounds **1** and **3** and then treated and untreated control cells were irradiated by light with $\lambda \geq 400$ nm and evaluated by viability, apoptosis and proliferation assay. The results obtained in our evaluation of the photodynamic activity of **1** and **3** against Hep-2 cells are presented in Fig. S15-16. It was shown that Hep-2 cells treated by **1** in concentration 500 μg/mL have 7±1.3% of dead cells after light irradiation, while dead cells were detected neither in control group nor in the cells treated by **3** Thus, such an approach is very promising to apply in photodynamic therapy using clusters with more intense luminescence as well as by prolonging time of irradiation or against special forms of cancer.

4 Conclusions

Two approaches to introduce photoactive hexanuclear molybdenum cluster complexes into the mesoporous metal-organic framework MIL-101 have been applied. The first approach was based on classical guest inclusion technique; the second one consisted in the post-synthetic modification of the conventional MIL-101 matrix by the substitution of pyrazine for aqua ligands at chromium atoms and then strong binding with the hexamolybdenum cluster complexes through the ditopic pyrazine strut. The modified solids have kept the structure and porosity of the pristine framework and demonstrated typical for hexamolybdenum cluster complexes red long-lived photoluminescence, which is responsible for reactive oxygen species generation typical for hexamolybdenum clusters. The special attention was paid to stability of materials obtained towards aqueous solutions. Thus, the behavior of soluble hexamolybdenum clusters with apical nitrate ligands as well as cluster doped MIL-101 in aqueous solutions was investigated. Rapid hydrolysis resulted in substitution of nitrates by water and hydroxyl ligands and forming a number of aquahydroxo complexes has been established by comparison of ESI-MS experimental and simulated spectra.

More importantly that at biological pH cluster complexes precipitate from the solution what is limiting of their application for photodynamic therapy. Whereas confocal microscopy confirmed that MIL-101 performed as a nanocarrier for octahedral metal cluster complexes, that could penetrate through the cellular membrane from MIL-101 nanoparticles adhered to the external surface of the cell, though in the case of strongly bonded cluster complexes to MIL-101-pyz matrix *via* pyrazine ligand the penetration does not occur.

The MTT study revealed a low cytotoxicity of pristine chromium metal-organic framework and molybdenum cluster inclusion compounds both with and without pyrazine strut. The optimal concentration of the cluster-containing materials for biological application was established to be at a level below 62.5 μg/mL. Furthermore, photoinduced reactive oxygen species generation in living cells by the released from MIL-101 cluster complexes was established. Also, we have demonstrated the ability of such a type of materials to apply in photodynamic therapy. The values obtained are not very high but significant, so we believe that the approach described is prospective and should lead to a new family of efficient materials for photodynamic treatment.

Acknowledgements

The synthesis of new compounds, their characterization by analytical and physical methods in this work were supported by RF government (Grant No. 14.Z50.31.006, leading scientist Martin Schröder). Biological properties study was supported by the Russian Foundation for Basic Research (Grant No. 14-04-01816). M.A. Shestopalov acknowledges the grant of the President of the Russian Federation (grant number MK 4054.2015.3) for financial support. Y. A. Vorotnikov and K. A. Brylev gratefully thank Prof. N. Kitamura (Hokkaido University) for the opportunity to study the luminescence properties. This work involved the use of equipment from the Multi-Access Center “Proteomics” of the Institute of Molecular Biology and Biophysics (Novosibirsk, Russia).

References

[1] S. Cordier, F. Grasset, Y. Molard, M. Amela-Cortes, R. Boukherroub, S. Ravaine, M. Mortier, N. Ohashi, N. Saito, H. Haneda, J Inorg Organomet P. 25 (2015) 189-204. doi:10.1007/s10904-014-0112-2.
[2] K. Kirakci, P. Kubat, K. Fejfarova, J. Martincik, M. Nikl, K. Lang, Inorg Chem. 55 (2016) 803-809. doi:10.1021/acs.inorgchem.5b02282.
[3] O.A. Efremova, K.A. Brylev, Y.A. Vorotnikov, L. Vejsadova, M.A. Shestopalov, G.F. Chimonides, P. Mikes, P.D. Topham, S.J. Kim, N. Kitamura, A.J. Sutherland, J Mater Chem C. 4 (2016) 497-503. doi:10.1039/c5tc03204k.
[4] M. Amela-Cortes, S. Paofai, S. Cordier, H. Folliot, Y. Molard, Chem Commun. 51 (2015) 8177-8180. doi:10.1039/c5cc01867f.
[5] K. Kirakci, P. Kubat, M. Dusek, K. Fejfarova, V. Sicha, J. Mosinger, K. Lang, Eur J Inorg Chem. (2012) 3107-3111. doi:10.1002/ejic.201200402.
[6] M.N. Sokolov, M.A. Mihailov, E.V. Peresypkina, K.A. Brylev, N. Kitamura, V.P. Fedin, Dalton T. 40 (2011) 6375-6377. doi:10.1039/c1dt10376h.
[7] M.A. Mikhailov, K.A. Brylev, P.A. Abramov, E. Sakuda, S. Akagi, A. Ito, N. Kitamura, M.N. Sokolov, Inorg Chem. 55 (2016) 8437–8445. doi:10.1021/acs.inorgchem.6b01042.
[8] A.O. Solovieva, Y.A. Vorotnikov, K.E. Trifonova, O.A. Efremova, A.A. Krasilnikova, K.A. Brylev, E.V. Vorontsova, P.A. Avrorov, L.V. Shestopalova, A.F. Poveshchenko, Y.V. Mironov, M.A. Shestopalov, J. Mater. Chem. B. 4 (2016) 4839-4846. doi:10.1039/C6TB00723F.
[9] K. Kirakci, V. Sicha, P. Holub, K. Lang, Inorg Chem. 53 (2014) 13012-13018. doi:10.1021/ic502144z.
[10] K. Kirakci, K. Fejfarova, M. Kucerakova, K. Lang, Eur J Inorg Chem. (2014) 2331-2336. doi:10.1002/ejic.201402076.
[11] J.A. Jackson, M.D. Newsham, C. Worsham, D.G. Nocera, Chem. Mater. 8 (1996) 558-564. doi:10.1021/cm950443f.
[12] A. Beltran, M. Mikhailov, M.N. Sokolov, V. Perez-Laguna, A. Rezusta, M.R. Revillo, F. Galindo, j. Mater. Chem. B. 4 (2016) 5975-5979. doi:10.1039/c6tb01966h.
[13] P. Agostinis, K. Berg, K.A. Cengel, H. Foster, A.W. Girotti, S.O. Gollnick, S.M. Hahn, M.R. Hamblin, A. Juzeniene, D. Kessel, M. Korbelik, J. Moan, P. Mroz, D. Nowis, J. Piette, B.C. Wilson, J. Golab, CA: Cancer J. Clin. 61 (2011) 250-281. doi:10.3322/caac.20114.
[14] A.P. Castano, P. Mroz, M.R. Hamblin, Nat Rev Cancer. 6 (2006) 535-545. doi:10.1038/nrc1894.
[15] K.Y. Choi, G. Liu, S. Lee, X.Y. Chen, Nanoscale. 4 (2012) 330-342. doi:10.1039/c1nr11277e.
[16] K. Kirakci, P. Kubat, M. Kucerakova, V. Sicha, H. Gbelcova, P. Lovecka, P. Grznarova, T. Ruml, K. Lang, Inorg Chim Acta. 441 (2016) 42-49. doi:10.1016/j.ica.2015.10.043.
[17] J. Elistratova, V. Burilov, A. Mustafina, M. Mikhailov, M. Sokolov, V. Fedin, A. Konovalov, Polymer. 72 (2015) 98-103. doi:10.1016/j.polymer.2015.07.010.
[18] J. Elistratova, M. Mikhailov, V. Burilov, V. Babaev, I. Rizvanov, A. Mustafina, P. Abramov, M. Sokolov, A. Konovalov, V. Fedin, Rsc Adv. 4 (2014) 27922-27930. doi:10.1039/c4ra02457e.
[19] A.A. Krasilnikova, A.O. Solovieva, K.E. Trifonova, K.A. Brylev, A.A. Ivanov, S.-J. Kim, M.A. Shestopalov, M.S. Fufaeva, A.M. Shestopalov, Y.V. Mironov, A.F. Poveshchenko, L.V. Shestopalova, Contrast Media Mol. Imaging. (2016). doi:10.1002/cmmi.1707.
[20] A.A. Krasilnikova, M.A. Shestopalov, K.A. Brylev, I.A. Kirilova, O.P. Khripko, K.E. Zubareva, Y.I. Khripko, V.T. Podorognaya, L.V. Shestopalova, V.E. Fedorov, Y.V. Mironov, J Inorg Biochem. 144 (2015) 13-17. doi:10.1016/j.jinorgbio.2014.12.016.
[21] M.A. Shestopalov, K.E. Zubareva, O.P. Khripko, Y.I. Khripko, A.O. Solovieva, N.V. Kuratieva, Y.V. Mironov, N. Kitamura, V.E. Fedorov, K.A. Brylev, Inorg Chem. 53 (2014) 9006-9013. doi:10.1021/ic500553v.

[22] S.J. Choi, K.A. Brylev, J.Z. Xu, Y.V. Mironov, V.E. Fedorov, Y.S. Sohn, S.J. Kim, J.H. Choy, J. Inorg. Biochem. 102 (2008) 1991-1996. doi:10.1016/j.jinorgbio.2008.07.013.
[23] N.A. Vorotnikova, O.A. Efremova, A.R. Tsygankova, K.A. Brylev, M.V. Edeleva, O.G. Kurskaya, A.J. Sutherland, A.M. Shestopalov, Y.V. Mironov, M.A. Shestopalov, Polym. Adv. Technol. 27 (2016) 922-928. doi:10.1002/pat.3749.
[24] M. Amela-Cortes, Y. Molard, S. Paofai, A. Desert, J.L. Duvail, N.G. Naumov, S. Cordier, Dalton T. 45 (2016) 237-245. doi:10.1039/c5dt03734d.
[25] O.A. Efremova, M.A. Shestopalov, N.A. Chirtsova, A.I. Smolentsev, Y.V. Mironov, N. Kitamura, K.A. Brylev, A.J. Sutherland, Dalton T. 43 (2014) 6021-6025. doi:10.1039/c3dt53126k.
[26] Y. Molard, F. Dorson, K.A. Brylev, M.A. Shestopalov, Y. Le Gal, S. Cordier, Y.V. Mironov, N. Kitamura, C. Perrin, Chem-Eur J. 16 (2010) 5613-5619. doi:10.1002/chem.200902131.
[27] Y.A. Vorotnikov, M.A. Mikhailov, K.A. Brylev, D.A. Piryazev, N.V. Kuratieva, M.N. Sokolov, Y.V. Mironov, M.A. Shestopalov, Russ. Chem. Bull., Int. Ed. 64 (2015) 2591-2596. doi:10.1007/s11172-015-1194-x.
[28] M. Kubeil, H. Stephan, H.J. Pietzsch, G. Geipel, D. Appelhans, B. Voit, J. Hoffmann, B. Brutschy, Y.V. Mironov, K.A. Brylev, V.E. Fedorov, Chem-Asian J. 5 (2010) 2507-2514. doi:10.1002/asia.201000284.
[29] Y.A. Vorotnikov, O.A. Efremova, N.A. Vorotnikova, K.A. Brylev, M.V. Edeleva, A.R. Tsygankova, A.I. Smolentsev, N. Kitamura, Y.V. Mironov, M.A. Shestopalov, Rsc Adv. 6 (2016) 43367-43375. doi:10.1039/C6RA04321F.
[30] T. Aubert, F. Cabello-Hurtado, M.A. Esnault, C. Neaime, D. Lebret-Chauvel, S. Jeanne, P. Pellen, C. Roiland, L. Le Polles, N. Saito, K. Kimoto, H. Haneda, N. Ohashi, F. Grasset, S. Cordier, J Phys Chem C. 117 (2013) 20154-20163. doi:10.1021/jp405836q.
[31] L. Gao, M.A. Peay, T.G. Gray, Chem. Mater. 22 (2010) 6240-6245. doi:10.1021/cm101609p.
[32] T. Aubert, A.Y. Ledneva, F. Grasset, K. Kimoto, N.G. Naumov, Y. Molard, N. Saito, H. Haneda, S. Cordier, Langmuir. 26 (2010) 18512-18518. doi:10.1021/la103784v.
[33] T. Aubert, F. Grasset, S. Mornet, E. Duguet, O. Cador, S. Cordier, Y. Molard, V. Demange, M. Mortier, H. Haneda, J Colloid Interf Sci. 341 (2010) 201-208. doi:10.1016/j.jcis.2009.09.064.
[34] F. Grasset, F. Dorson, S. Cordier, Y. Molard, C. Perrin, A.M. Marie, T. Sasaki, H. Haneda, Y. Bando, M. Mortier, Adv Mater. 20 (2008) 143-148. doi:10.1002/adma.200701686.
[35] A.M. Cheplakova, K.A. Kovalenko, M.A. Shestopalov, K.A. Brylev, V.P. Fedin, Russ. Chem. Bull. 63 (2014) 1487-1492. doi:10.1007/s11172-014-0624-5.
[36] K.A. Kovalenko, D.N. Dybtsev, S.F. Lebedkin, V.P. Fedin, Russ. Chem. Bull. 59 (2010) 741-744. doi:10.1007/s11172-010-0155-7.
[37] D. Dybtsev, C. Serre, B. Schmitz, B. Panella, M. Hirscher, M. Latroche, P.L. Llewellyn, S. Cordier, Y. Molard, M. Haouas, F. Taulelle, G. Férey, Langmuir. 26 (2010) 11283-11290. doi:10.1021/la100601a.
[38] K.A. Kovalenko, V.P. Fedin, Russ. Chem. Bull., Int. Ed. 65 (2016) 1406-1417.
[39] P. Horcajada, C. Serre, G. Maurin, N. Ramsahye, F. Balas, M. Vallet-Regí, M. Sebban, F. Taulelle, G. Férey, J. Am. Chem. Soc. 130 (2008) 6774-6780. doi:10.1021/ja710973k.
[40] P. Horcajada, C. Serre, M. Vallet-Regí, M. Sebban, F. Taulelle, G. Férey, Angew. Chem. Int. Ed. 45 (2006) 5974-5978. doi:10.1002/anie.200601878.
[41] V. Rodriguez-Ruiz, A. Maksimenko, R. Anand, S. Monti, V. Agostoni, P. Couvreur, M. Lampropoulou, K. Yannakopoulou, R. Gref, J Drug Target. 23 (2015) 759-767. doi:10.3109/1061186X.2015.1073294.
[42] P. Horcajada, R. Gref, T. Baati, P.K. Allan, G. Maurin, P. Couvreur, G. Férey, R.E. Morris, C. Serre, Chem. Rev. 112 (2012) 1232-1268. doi:10.1021/cr200256v.
[43] F. Ke, Y.-P. Yuan, L.-G. Qiu, Y.-H. Shen, A.-J. Xie, J.-F. Zhu, X.-Y. Tian, L.-D. Zhang, J. Mater. Chem. 21 (2011) 3843-3848. doi:10.1039/c0jm01770a.

[44] P. Horcajada, T. Chalati, C. Serre, B. Gillet, C. Sebrie, T. Baati, J.F. Eubank, D. Heurtaux, P. Clayette, C. Kreuz, J.-S. Chang, Y.K. Hwang, V. Marsaud, P.-N. Bories, L. Cynober, S. Gil, G. Férey, P. Couvreur, R. Gref, Nat. Mater. 9 (2010) 172-178. doi:10.1038/nmat2608.
[45] K.M.L. Taylor-Pashow, J.D. Rocca, Z. Xie, S. Tran, W. Lin, J. Am. Chem. Soc. 131 (2009) 14261-14263. doi:10.1021/ja906198y.
[46] J. An, S.J. Geib, N.L. Rosi, J. Am. Chem. Soc. 131 (2009) 8376-8377. doi:10.1021/ja902972w.
[47] J. Wang, D. Chen, B. Li, J. He, D. Duan, D. Shao, M. Nie, Sci. Rep. 6 (2016) 26126. doi:10.1038/srep26126.
[48] G. Férey, C. Mellot-Draznieks, C. Serre, F. Millange, J. Dutour, S. Surblé, I. Margiolak, Science. 309 (2005) 2040-2042. doi:10.1126/science.1116275.
[49] J.N. Paczkowski, D.C., ACS Symp. Ser. 278 (1985) 222-242. doi:10.1021/bk-1985-0278.ch014.
[50] R.P. Taylor, J.B. Vatz, J. Am. Chem. Soc. 95 (1973) 5819-5820. doi:10.1021/ja00798a093.
[51] Y. Lee, E. Shacter, J. Biol. Chem. 274 (1999) 19792-19798. doi:10.1074/jbc.274.28.19792.
[52] D.N. Dybtsev, K. Kovalenko, Y.V. Mironov, V.P. Fedin, G. Férey, N.A. Yakovleva, E.A. Berdonosova, S.N. Klyamkin, E.V. Kogan, Russ. Chem. Bull. 58 (2009) 1623-1626. doi:10.1007/s11172-009-0223-z.
[53] K.A. Kovalenko, A.M. Cheplakova, P.V. Burlak, V.P. Fedin, Russ. J. Inorg. Chem. 60 (2015) 790-794. doi:10.1134/S0036023615070086.
[54] S. Roy, S. Choubey, K. Bhar, S. Khan, P. Mitra, B.K. Ghosh, J. Mol. Struct. 1051 (2013) 328-335. doi:10.1016/j.molstruc.2013.08.016.
[55] S.A. Sapchenko, D.N. Dybtsev, D.G. Samsonenko, V.P. Fedin, New J. Chem. 34 (2010) 2445-2450. doi:10.1039/C0NJ00196A.
[56] M.D. Allendorf, C.A. Bauer, R.K. Bhakta, R.J.T. Houk, Chem. Soc. Rev. 38 (2009) 1330-1352. doi:10.1039/B802352M.
[57] L.S. Forster, Coord. Chem. Rev. 248 (2004) 261-272. doi:10.1016/j.ccr.2003.10.014.
[58] M.A. Mikhailov, K.A. Brylev, A.V. Virovets, M.R. Gallyamov, I. Novozhilov, M.N. Sokolov, New J. Chem. 40 (2016) 1162-1168. doi:10.1039/c5nj02246k.
[59] M.N. Sokolov, M.A. Mikhailov, K.A. Brylev, A.V. Virovets, C. Vicent, N.B. Kompankov, N. Kitamura, V.P. Fedin, Inorg Chem. 52 (2013) 12477-12481. doi:10.1021/ic401377g.
[60] J.A. Jackson, C. Turro, M.D. Newsham, D.G. Nocera, J Phys Chem-Us. 94 (1990) 4500-4507. doi:10.1021/J100374a029.

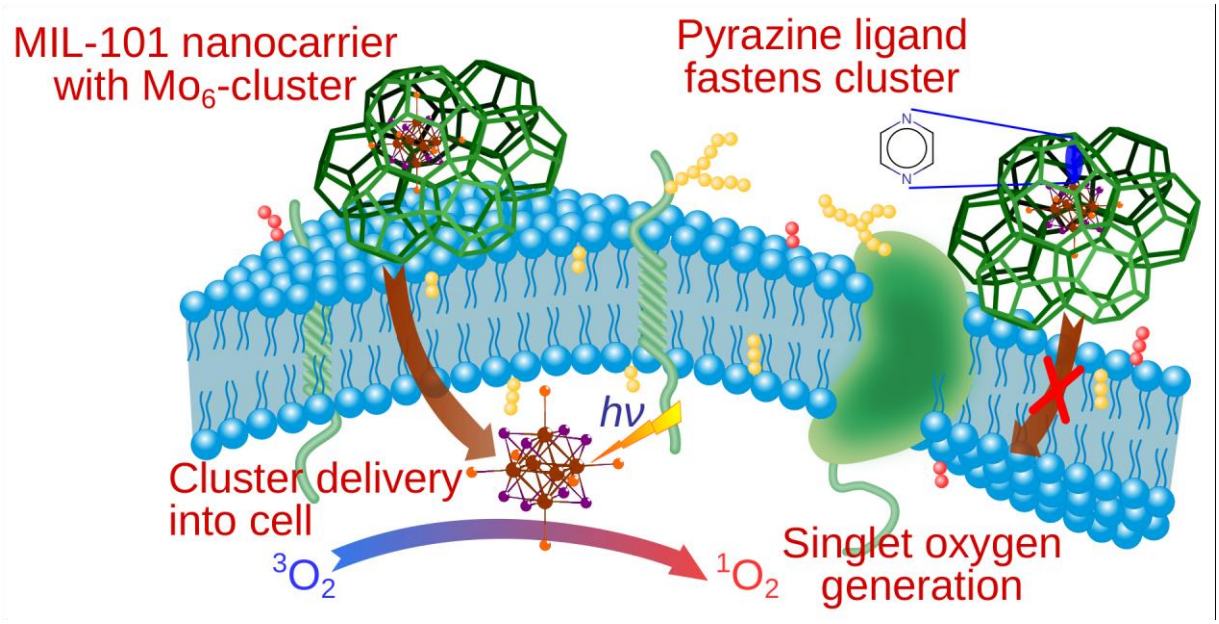

Graphical abstract

5 Synopsis

Hexamolybdenum clusters possessing red fluorescence were introduced into nanosized chromium terephthalate metal-organic framework. Clusters anchored *via* pyrazine cannot penetrate into cells whereas clusters from pyrazine-free compound transport through membrane and generate singlet oxygen in cancer Hep-2 cells. Thus, such system is a suitable nanocarrier for applications in photodynamic therapy.

6 Highlights

- Molybdenum clusters in mesoporous chromium terephthalate metal-organic framework
- Luminescence of hybrids were investigated and compared to clusters in solutions
- Cytotoxicity of all compounds were established at low level.
- Penetration of clusters into Hep-2 cells were observed for pyrazine-free compound.
- Generation of reactive oxygen species were tested *in vitro* and in living cells.